

Proceedings of the Korean Nuclear Society Autumn Meeting

Seoul, Korea, October 2001

## Development of ICRF System Components for KSTAR Tokamak

Bong Guen Hong, Young Dug Bae, Churl Kew Hwang, Jong Gu Kwak,

and Jae Sung Yoon

Korea Atomic Energy Research Institute

150 Dukjin-Dong, Yusong-Ku, Taejon 305-353, Korea

### Abstract

The ICRF system for the KSTAR tokamak is being developed to support long-pulse, high- $\beta$ , advanced tokamak fusion physics experiments. The ICRF system will deliver 12 MW of rf power to the plasma for 300 seconds through two antennas located in adjacent ports. With the frequency range of 25 to 60 MHz, it provides heating for the plasmas, centrally peaked current drive, and off-axis current drive using mode-conversion for various operating scenarios over a range of magnetic fields. Steady-state relevant ICRF components have been developed in the area of the antenna, the vacuum feedthrough and the matching devices. In this work, rf test results with intermediate power at the frequency of  $\sim 30$  MHz are presented.

### 1. Introduction

The Korea Superconducting Tokamak Advanced Research (KSTAR) tokamak [1, 2] ( $R_0 = 1.8$  m,  $a = 0.5$  m,  $\kappa = 2$ ,  $\delta = 0.8$ ,  $B_T = 3.5$  T,  $I_p = 2$  MA,  $\tau_{\text{pulse}} = 300$  sec) is being constructed to perform long pulse, high  $\beta$ , advanced tokamak fusion physics experiments. The neutral beam (14 MW, 120 keV), the ion cyclotron (12 MW, 25 - 60 MHz), the lower hybrid (3 MW,  $\geq 5.0$  GHz) and the electron cyclotron (0.5 MW, 84 GHz) systems provide heating as well as current drive capability for a long pulse length of up to 300 sec. The systems also provide flexibility in the control of current density and pressure profiles for the study of advanced tokamak plasmas.

Heating and current drive using fast wave in the ion cyclotron range of frequencies

have been proposed as one of the main features for the advanced tokamak operation of KSTAR tokamak. The ICRF system initially delivers 6 MW of rf power to the plasma using a single four-strap antenna mounted in a midplane port and will be capable of 300 sec operation with 12 MW of rf power to the plasma through two antennae located in adjacent ports. The ICRF system is designed to meet the requirements that it operate at any frequency in the range of 25 – 60 MHz and it operate for long pulse length up to 300 seconds. The ICRF system provides heating for the plasmas, centrally peaked current drive, and off-axis current drive using mode-conversion for various operating scenarios over a range of magnetic fields,  $B_T = 2.5 - 3.5$  T. For  $B_T = 3.5$  T, the frequency of  $\sim 50$  MHz is good for H minority heating or second harmonic heating of D in D majority plasma. The frequency of  $\sim 38$  MHz can be used as an on-axis fast wave current drive (FWCD) scheme for a steady-state operation of KSTAR. With a  $\text{He}^3$  minority, operation between 30 MHz and 40 MHz may be possible for  $\text{He}^3$  minority heating or off-axis current drive using mode-conversion. The capability of changing the current drive efficiency to control the current density profile is provided by changing the phasing between the antenna strap currents during operation. [3]

For long pulse, high power operation of KSTAR ICRF system, efforts have been made to develop key ICRF technologies; A prototype ICRF antenna of 6 MW rf power and a vacuum feedthrough of 1 MW rf power have been developed. To remove the dissipated rf power loss, cooling paths were carefully designed. For reliable operation during high power transmission, the matching devices such as liquid stub and liquid phase shifter are developed. Stub using liquid instead of gas for insulating dielectric medium have been found reliable compared to the conventional stub in LHD experiments. [4]

## 2. KSTAR ICRF System

A schematic of the KSTAR ICRF system is shown in Fig. 1. An antenna composed of four current straps side by side, each of which is grounded at the center and has a coaxial feed line connected to each end of the current strap. A resonant double loop consists of vacuum transmission line, vacuum feedthrough and pressurized coaxial line with two adjustable phase shifters to cover any frequency in the range of 25 – 60 MHz. The ICRF system delivers 6 MW of power to the plasma without exceeding 35 kV anywhere in the loop for various heating and current drive scenarios. Three decouplers between the neighboring strap circuits are required to balance the power needed from each rf source. A matching system consists of a phase shifter and a stub tuner in each of

the four lines driving the current strap resonant loops. As an optional upgrade, a combiner/splitter circuit that acts as an "ELM dump" circuit when the current straps are driven with  $\pi/2$  inter-strap phasing for FWCD will be considered. The phasing between current straps in the antenna will be adjustable quickly during operation to provide the capability of changing the current drive efficiency. Fig. 2 shows the variation of the absolute value of the reflection coefficient ( $\rho$ ) for each line after the decouplers with the system component values set up for zero reflection at  $\pi/2$  phasing which corresponds to the fast wave current drive scenario at 38 MHz (with plasma loading of  $6 \Omega$  assumed). As the phase angle deviates from  $\pi/2$ ,  $\rho$  departs from zero on all the lines, but in the worst case,  $\rho$  is less than 0.08 corresponding to less than 1% reflected power toward the transmitters. Four rf sources cover the frequency range of 25 – 60 MHz and can deliver up to 2 MW into a matched load. The analysis also shows that for the plasma loading change of  $4 - 8 \Omega$  with tuners set to  $6 \Omega$ , the VSWR (Voltage Standing Wave Ratio) can be kept within 1.5.

### 3. ICRF System Components Development

The antenna is constrained to be 830 mm high and 730 mm wide in order to fit through the port. Inside the vacuum vessel, the front surface of the Faraday shield is located 2 cm outside the flux surface of the reference equilibrium. To protect the antenna, wall mounted poloidal limiters made of CFC tiles are located on both sides of the antenna. The antenna structure is radially movable under vacuum (but not during a shot) so that the antenna position relative to the plasma can be adjusted to optimize the power coupled to the plasma. For 300 seconds operation, the antenna has many cooling channels inside the current strap, Faraday shield, cavity wall and vacuum transmission line to remove the dissipated rf power loss and incoming plasma heat loads. The Faraday shield is made of Cu plated and  $B_4C$  coated Inconel 625 tube. The thermal and stress analysis during normal and transient operation conditions show that the maximum stresses in the Faraday shield tube and in the current strap are below the allowable level.

A prototype ICRF antenna was fabricated and is shown in Fig. 3. In the prototype antenna, SUS tube is used for the Faraday shield material instead of  $B_4C$  coated Inconel 625 and Viton O-ring is used for sealing material instead of Helicoflex type. Thus baking temperature is limited up to about 100 °C. The antenna is installed in the RF test chamber evacuated by 2000 l/s turbomolecular pump and the mechanical tests have been performed. The flow rates of the cooling water in the Faraday shield tube and current strap was found to be 1.6 m/sec and 3.6 m/sec, respectively, and radial motion

under vacuum was found to be 4 mm/sec with  $\pm 0.1$  mm position accuracy. The test results satisfy the mechanical requirements of the KSTAR antenna. Electrical characteristics such as mutual coupling, vacuum impedance and field patterns in front of the antenna, as well as the high voltage and the current behavior under no plasma load conditions, are investigated. With the half of a current strap connected to the matching circuit via a vacuum feedthrough and a directional coupler, and the other seven ports shorted at the input ports, intermediate rf power test has been performed at  $f=32$  MHz. During the rf pulse, the maximum peak voltage, forward/reflected powers, temperature on the antenna and gas pressure are measured. The rf power test has been performed up to 23 kV at a pulse length of 87 sec. Time evolution of rf pulse, peak voltage and pressure is shown in Fig. 4. rf power was gradually increased, sustained to be constant, and stepwise terminated. The maximum voltage of the standing wave was limited by the output power of the amplifier and the circuit loss. The maximum peak voltage of 23 kV is equivalent to a 3.6 MW heating power with 6  $\Omega/m$  of expected plasma loading. The pulse length was limited by the overheating of the cavity wall. At the low RF power, reflected power is large because the multipactor discharge is occurred, and it is terminated above the rf power of 4.1 kW. There was a forbidden power band of 4 ~ 8 kW at the increasing phase of rf pulse due to the multipactor discharge. The gas pressure of RFTC increased up to  $2.2 \times 10^{-5}$  mbar during the rf pulse. At beginning phase of the rf pulse, multipactor discharge causes large increment of the pressure. After the multipactor is terminated, the pressure gradually increases by the outgassing from heated cavity wall, and it decreases as the cavity wall is conditioned by rf pulse.

The vacuum feedthrough for 1 MW rf power transmission is designed to have two alumina ( $\text{Al}_2\text{O}_3$ , 99.7 %) ceramic cylinders and an O-ring seal instead of a brazed seal for good mechanical and thermal strength. Fig. 5 shows a detailed design of the vacuum feedthrough. Calculations of the electric field and resulting rf dissipation power density show that with 30 kV imposed between inner and outer conductors,  $\sim 1$  kW power for conductor and  $\sim 150$  W power for ceramic need to be cooled. Independent inlet and outlet water cooling channels are installed to cool the inner conductor. For cooling of the ceramics, a gas ( $\text{N}_2$ ) is circulated in space between the two cylinders and the outer conductor. Electrical performance to investigate the effects of heating on the conductors and the insulators is evaluated. Fig. 6 shows time evolutions of RF pulse, the line voltage, the temperature, and the gas pressure. The forward power decreased and the reflected power increased gradually during the RF pulse, because the matching condition of the test circuit was shifted from optimum condition by the heating of the transmission line components. The maximum voltage of the standing wave was 32.2 kV

(peak) and the pulse length was extended to 300 sec with the temperature increase of only up to 43 (T<sub>0</sub>=30). From the experimental result, the tan of the ceramic is estimated to be 2 × 10<sup>-4</sup> which is satisfactorily low value. The maximum peak voltage of 30 kV is equivalent to a 0.8 MW transmission power (total power of 6.1 MW) to the antenna with 6 /m of expected plasma loading.

The liquid stub tuner and phase shifter use the difference between rf wavelength in liquid and in gas due to the different relative dielectric constant. They have no sliding contact and can withstand high rf voltage. We developed a 4 m long, 6" stub tuner and a U-shaped, 9" phase shifter with 130° phase variation at 30 MHz. Silicon oil was used as a liquid (dielectric constant, ε<sub>L</sub> = 2.72). Rf test (50 kW, 30 MHz) shows that they have a high stand-off voltage (> 40 kV) and they are reliable rf components for long pulse, high power transmission.

As future works, higher power and longer pulse test will be performed with some improvements based on the present test results.

#### 4. Summary

Design of the ICRF system for the KSTAR tokamak has been completed and efforts have been made to develop the long pulse relevant ICRF System components. Antenna, vacuum feedthrough, and key matching components for long pulse, high power transmission have been developed. The results of the design and the engineering development will make ICRF system a key component for the steady-state, high performance modes of KSTAR tokamak operation.

#### Acknowledgments

This work was supported by the Korean Ministry of Science and Technology under KSTAR Project Contract.

#### References

1. G.S. Lee et. al., *Nucl. Fusion* **40**, 575 (2000).
2. G.S. Lee et al., *Fusion Engineering and Design* **46**, 405-411 (1999).
3. C.K. Hwang, B.G. Hong and D. Swain, *Fusion Engineering and Design* **45**, 127 (1999).
4. R. Kumazawa et al., *Rev. Sci. Instrum.* **70**, 2665 (1999).

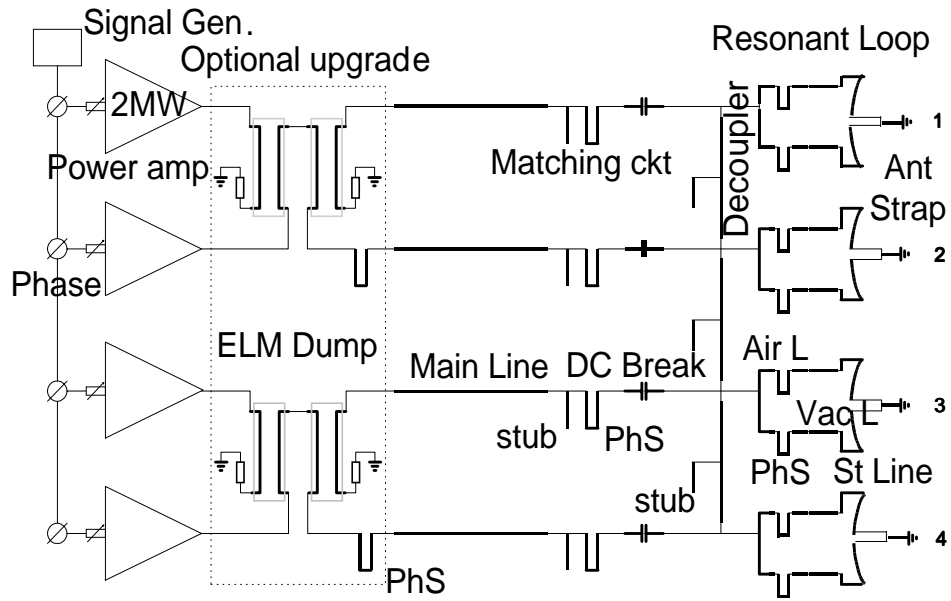


Fig. 1. Schematic of the KSTAR ICRF system

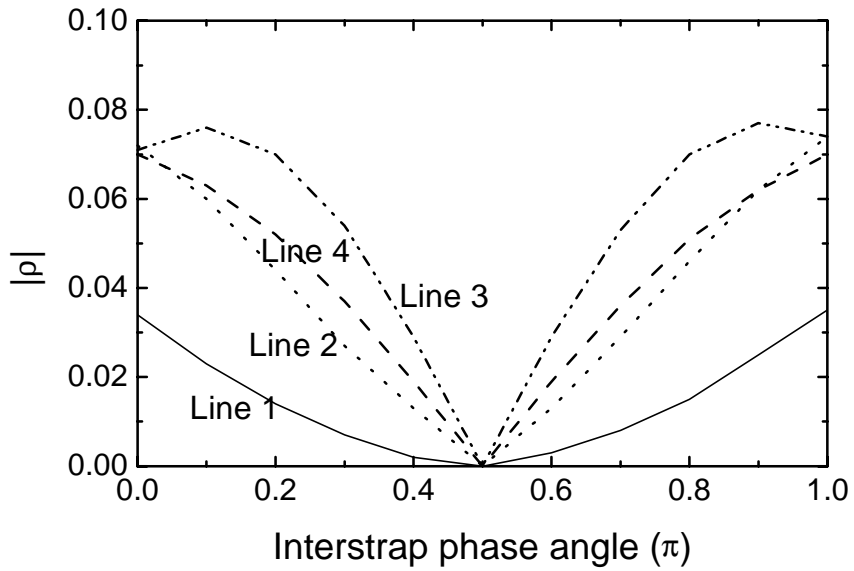


Fig. 2 Absolute value of the reflection coefficient vs. interstrap phase angle at 38 MHz

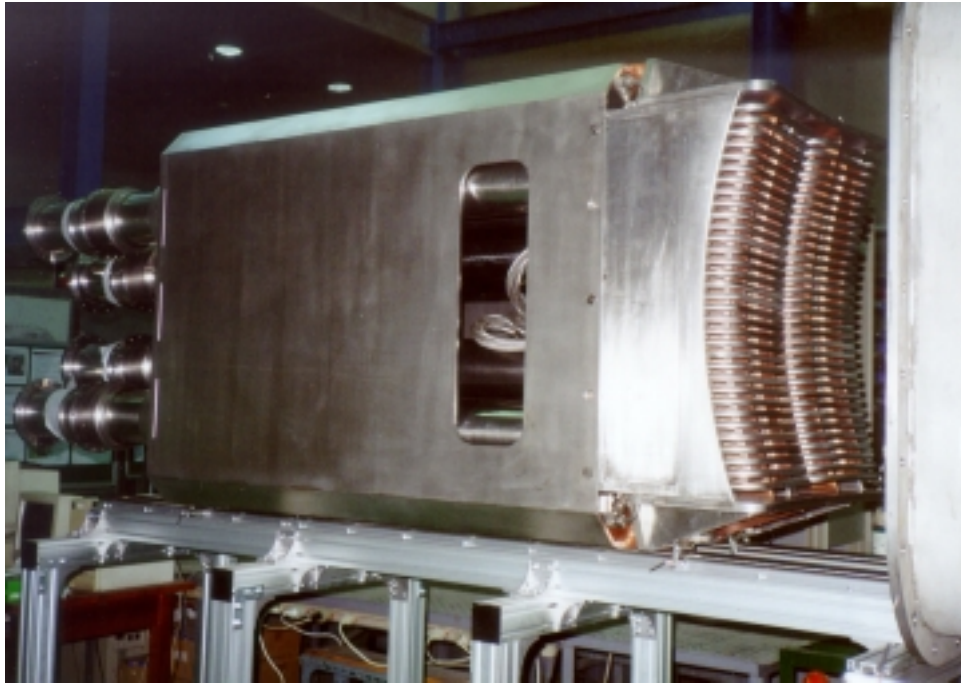


Fig. 3 A prototype ICRF antenna

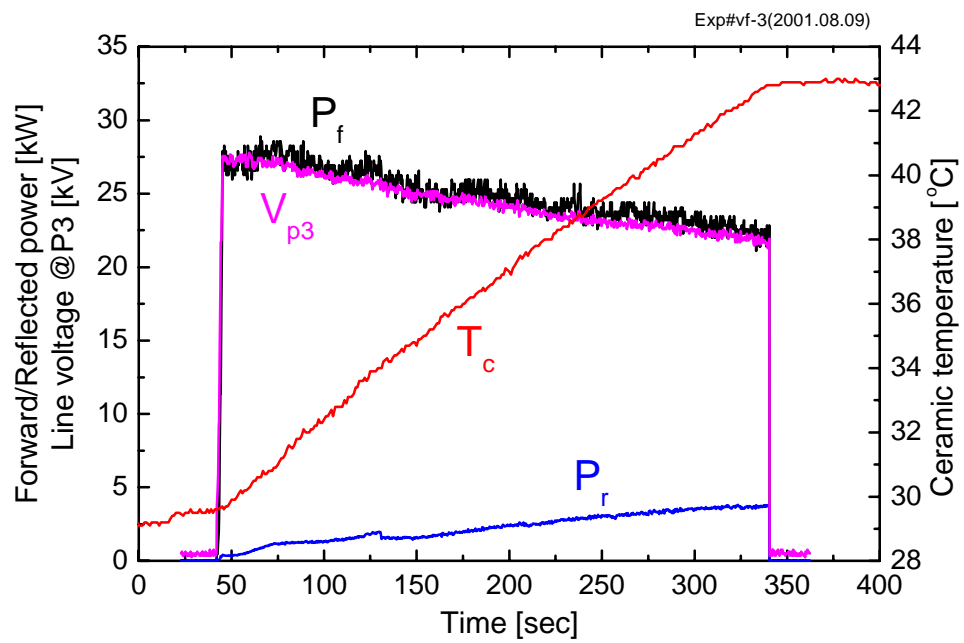


Fig. 4 Time evolution of rf pulse, peak voltage and pressure

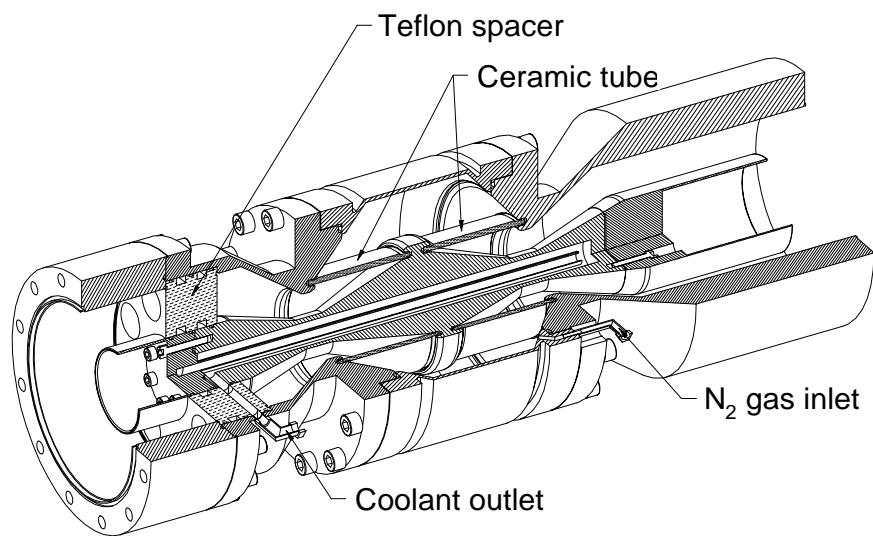


Fig. 5. Detailed drawing of the vacuum feedthrough

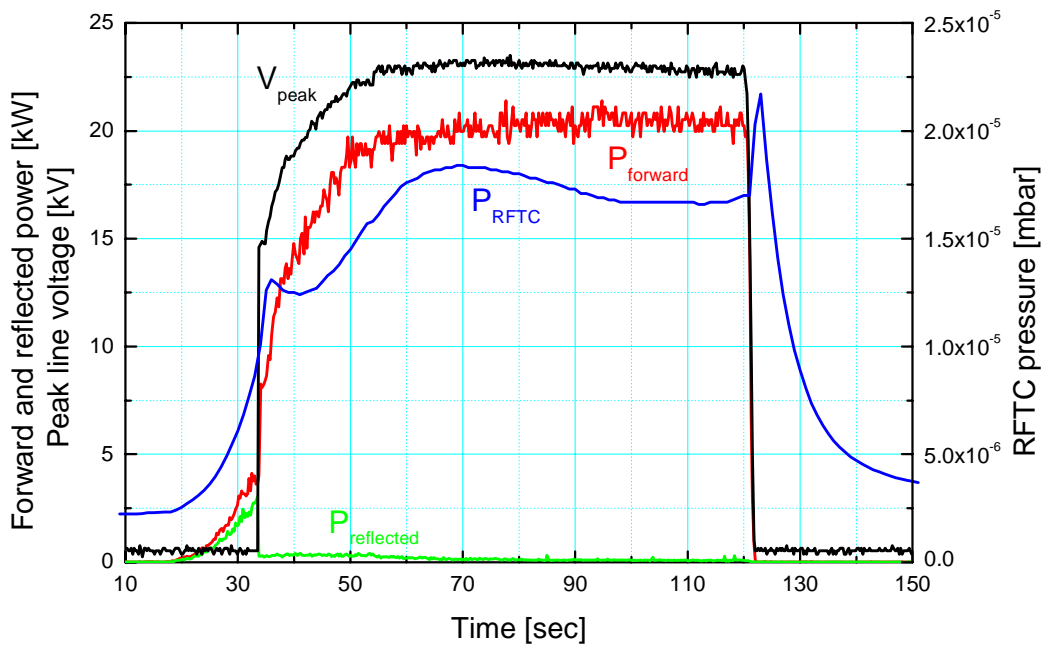


Fig. 6 Time evolutions of RF pulse, line voltage, temperature, and gas pressure